PHYSOR 2002, Seoul, Korea, October 7-10, 2002

COUPLING OF FORWARD AND ADJOINT MONTE CARLO CALCULATIONS FOR CONTINUOUS ENERGY BY NEXT-EVENT ESTIMATION

J.E. Hoogenboom and **D. Legrady**
Delft University of Technology, Interfaculty Reactor Institute
Mekelweg 15, 2629 JB Delft, The Netherlands
j.e.hoogenboom@iri.tudelft.nl ; d.legrady@iri.tudelft.nl

ABSTRACT

Coupling of forward and adjoint Monte Carlo calculations can be applied in several ways. Here we consider the coupling at a surface that divides the total problem space in a part containing the total neutron source and a part containing the detector. Up to now this coupling required a segmentation of the coupling surface in small areas, but also with respect to energy and directional intervals. In this paper it is described how the coupling can be realised for a continuous energy treatment of the neutron transport without any segmentation of the coupling surface. This requires the introduction of a next-event estimator to match not only the crossing point of the coupling surface for a forward and an adjoint history, but also the particle direction and energy.
Given a collision site of a forward particle at one side of the coupling surface and a collision site and direction and energy of an adjoint particle at the other side of the surface, the next-event estimator has to determine the next collision site for the adjoint particle such that it could have a collision thereafter at the collision site of forward particle, while its energy matches that of the forward particle.

1. INTRODUCTION

Forward Monte Carlo calculations may become impractical because of the bad statistics if the detector for which the response has to be calculated is small and/or at a relatively large distance from the source. In that case adjoint Monte Carlo may be helpful to get an acceptable standard deviation in a reasonable computing time. However, if also the source is small, an adjoint calculation will neither help. In that case there are several possibilities to combine a forward calculation, starting at the physical source and an adjoint calculation starting at the detector. A useful overview is given by Cramer [1]. One of the coupling methods uses a next-event estimator to couple forward and adjoint particles, forcing forward and adjoint particles to have the same collision site and the same flight direction. This method was demonstrated by Ueki et al.[2] for the case of a multigroup treatment. In that case the additional condition of equal energy group number for the next-event estimation can rather easily be met.
Now that calculation possibilities are available for adjoint Monte Carlo in continuous-energy mode, it also becomes of interest to develop a continuous-energy form of the next-event coupling method. However, the coupling requirement that the forward and the adjoint particle must be at the same site, have the same direction and the same energy cannot be met by introducing one additional collision event. Introducing two consecutive collisions in the adjoint calculation, however, offers the possibility of exactly fulfilling the coupling condition.

2. THEORY

The neutron or photon transport equation in integro-differential form reads

$$\boldsymbol{\Omega}\cdot\nabla\phi+\boldsymbol{\Sigma}_t\phi=\iint\boldsymbol{\Sigma}_s(\boldsymbol{r},E'\to E,\boldsymbol{\Omega}'\to\boldsymbol{\Omega})\phi(\boldsymbol{r},E',\boldsymbol{\Omega}')dE'd\Omega'+S \tag{1}$$

We denote the quantity to be calculated as R, which can we written as an average over the particle flux with a detector response function D as follows

$$R=\int D(P)\phi(P)dP \tag{2}$$

with P denoting a point in the phase space P=($\boldsymbol{r}$,E,$\boldsymbol{\Omega}$). The adjoint equation reads

$$-\boldsymbol{\Omega}\cdot\nabla\phi^+ +\boldsymbol{\Sigma}_t\phi^+=\iint\boldsymbol{\Sigma}_s(\boldsymbol{r},E\to E',\boldsymbol{\Omega}\to\boldsymbol{\Omega}')\phi^+(\boldsymbol{r},E',\boldsymbol{\Omega}')dE'd\Omega'+D \tag{3}$$

which allows the detector response R to be written as an integral over the adjoint function times the particle source density. If we divide the volume V of the total system in two parts by a surface A (Fig. 1),

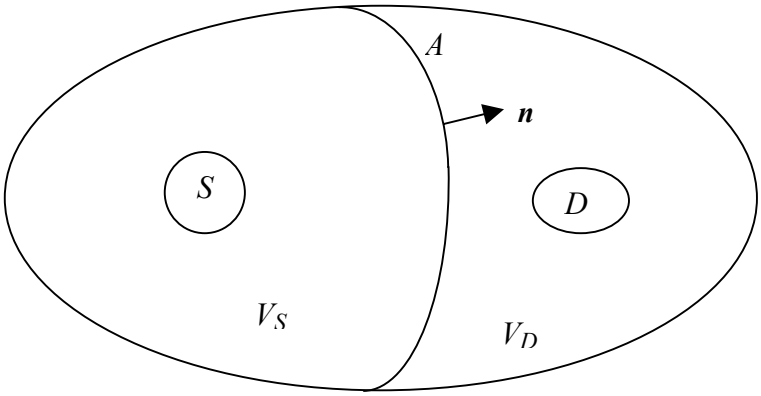

Fig. 1. Division of source-detector system in volume V_S and V_D by surface A

such that one part V_S contains the full source S and the other part V_D the full detector, we can derive a third form of obtaining the detector response. Multiplying Eq.(1) by ϕ^+ and Eq.(3) by ϕ, subtracting the result and integrating over the volume V_D only, over all directions and energies, and using the zero incoming flux and zero outgoing adjoint function at the system outer boundary we get [3]

$$R=\int D(P)\phi(P)dP=\int S(P)\phi^+(P)dP=\int_A\boldsymbol{n}\cdot\boldsymbol{\Omega}\phi(P)\phi^+(P)dP_A \tag{4}$$

with in the last term the integration over the surface enclosing the volume V_D instead of the system volume. This last expression can be interpreted in a Monte Carlo sense as follows[3]. Perform a forward Monte Carlo calculation with particles starting at the source and giving a score when they cross the surface A equal to the particle current $\boldsymbol{n}\cdot\boldsymbol{\Omega}\,\phi$. Next perform an adjoint Monte Carlo calculation, thus starting particle histories at the detector, and recording scores equal to the adjoint particle flux ϕ^+ when they cross the surface A in either direction. The scores of the forward and the adjoint histories belonging to the same small surface segment on A, the same small energy range and the same small directional interval

are multiplied and the result summed over all intervals[3]. This is one way of coupling forward and adjoint Monte Carlo calculations and was called the midway method.

We now introduce a disturbed system in the sense that for the adjoint calculation the volume V_S contains a pure absorber with the total cross section equal to that for the unperturbed system. Then the adjoint equation for the perturbed adjoint function $\tilde{\phi}^+$ is

$$-\boldsymbol{\Omega}\cdot\nabla\tilde{\phi}^+ + \boldsymbol{\Sigma}_t\tilde{\phi}^+ = \begin{cases} \iint \boldsymbol{\Sigma}_s(\boldsymbol{r}, E\to E', \boldsymbol{\Omega}\to\boldsymbol{\Omega}')\tilde{\phi}^+(\boldsymbol{r}, E', \boldsymbol{\Omega}')dE'd\Omega' + D & \boldsymbol{r}\in V_D \\ 0 & \boldsymbol{r}\in V_S \end{cases} \tag{5}$$

Using the same procedure as before we can prove

$$R = \int_A \boldsymbol{n}\cdot\boldsymbol{\Omega}\phi(P)\tilde{\phi}^+(P)dP_A \tag{6}$$

This means that the requested detector response R of the unperturbed system can also be obtained by coupling a forward Monte Carlo calculation for the unperturbed system with an adjoint Monte Carlo calculation of the perturbed system. In fact, the perturbation need not to be a pure absorber, but may be any perturbation in V_D[3]. A pure absorber perturbation has the advantage that adjoint particles crossing the surface A and thus entering the pure absorber zone cannot scatter back to the surface A to make another score and thus need not to be followed any longer, reducing the computation time.

The disadvantage of this type of coupling of the forward and adjoint calculations is that it requires a discretization of all variables at the surface A to calculate the coupled score.

To eliminate this disadvantage a next-event estimator was proposed by Ueki et al. [2], whose technique only applies to a multigroup treatment of the transport process. For application to a continuous energy treatment further extensions are needed. To derive the required theorem we again multiply Eq.(1) by $\tilde{\phi}^+$ and Eq.(3) by ϕ subtract both equations and integrate over all energies and directions, but now only over the volume V_S instead of V_D. This leads to

$$\begin{gathered} R = \int_A \boldsymbol{n}\cdot\boldsymbol{\Omega}\phi(P)\tilde{\phi}^+(P)dP_A = \\ \int_{V_S} S(P)\tilde{\phi}^+(P)dP + \int_{V_S}\tilde{\phi}^+(P)dP\iint \boldsymbol{\Sigma}_s(\boldsymbol{r}, E'\to E, \boldsymbol{\Omega}'\to\boldsymbol{\Omega})\phi(\boldsymbol{r}, E', \boldsymbol{\Omega}')dE'd\Omega'dP \end{gathered} \tag{7}$$

Before we can proceed we have to consider the actual Monte Carlo simulation of the forward and adjoint transport equation. For a Monte Carlo simulation the integro-differential form of the transport equation is not suited. We therefore consider the integral form of the forward transport equation in the form [4]

$$\psi(P) = \boldsymbol{\Sigma}_t(P)\phi(P) = \int T(\boldsymbol{r'}\to\boldsymbol{r}, E, \boldsymbol{\Omega})\chi(\boldsymbol{r'}, E, \boldsymbol{\Omega})dV' \tag{8}$$

with $\psi(P)$ the collision density, which is directly related to the particle flux from the integro-differential description, and $\chi(P)$ the emission density given by

$$\chi(P) = S(P) + \iint C(\boldsymbol{r}, E'\to E, \boldsymbol{\Omega}'\to\boldsymbol{\Omega})\psi(\boldsymbol{r}, E', \boldsymbol{\Omega}')dE'd\boldsymbol{\Omega}' \tag{9}$$

The transport kernel $T(\boldsymbol{r}'\rightarrow\boldsymbol{r})$ gives the probability for a particle at $\boldsymbol{r}'$ to have its next collision at $\boldsymbol{r}$. The collision density $C(E'\rightarrow E,\boldsymbol{\Omega}'\rightarrow\boldsymbol{\Omega})$ is given by

$$C(\boldsymbol{r},E'\rightarrow E,\boldsymbol{\Omega}'\rightarrow\boldsymbol{\Omega})=\frac{\boldsymbol{\Sigma}_s(\boldsymbol{r},E'\rightarrow E,\boldsymbol{\Omega}'\rightarrow\boldsymbol{\Omega})}{\boldsymbol{\Sigma}_t(\boldsymbol{r},E')} \tag{10}$$

The adjoint Monte Carlo simulation should be based on the equations adjoint to Eqs.(8) and (9), introducing the adjoint functions ψ^+ and χ^+. However, for a suitable Monte Carlo simulation a transformation is needed, leading to the following equations[4] for the adjoint collision density

$$\xi^+(P)=\boldsymbol{\Sigma}_t(P)\chi^+(P)=\int T^+(\boldsymbol{r}'\rightarrow\boldsymbol{r},E,\boldsymbol{\Omega})\zeta^+(\boldsymbol{r}',E,\boldsymbol{\Omega})dV' \tag{11}$$

and the adjoint emission density

$$\zeta^+(P)=D(P)+\iint P^+(\boldsymbol{r},E')C^+(\boldsymbol{r},E'\rightarrow E,\boldsymbol{\Omega}'\rightarrow\boldsymbol{\Omega})\xi^+(\boldsymbol{r},E',\boldsymbol{\Omega}')dE'd\Omega' \tag{12}$$

Here C^+ is the (normalized) adjoint collision density and P^+ the analogon of the non-absorption probability, which is taken into account as a factor multiplying the statistical weight of the adjoint particle. The connection with adjoint function ϕ^+ of the integro-differential form of the adjoint equation (3) is given by $\chi^+=\phi^+$ or $\xi^+=\Sigma_t\phi^+$.
The perturbed adjoint problem is described by

$$\tilde{\xi}^+(P)=\int T^+(\boldsymbol{r}'\rightarrow\boldsymbol{r},E,\boldsymbol{\Omega})\tilde{\xi}^+(\boldsymbol{r}',E,\boldsymbol{\Omega})dV' \tag{13}$$

and

$$\tilde{\xi}^+(P)=\begin{cases}D(P)+\iint P^+(\boldsymbol{r},E')C^+(\boldsymbol{r},E'\rightarrow E,\boldsymbol{\Omega}'\rightarrow\boldsymbol{\Omega})\tilde{\xi}^+(\boldsymbol{r},E',\boldsymbol{\Omega}')dE'd\Omega' & \boldsymbol{r}\in V_D\\ 0 & \boldsymbol{r}\in V_S\end{cases} \tag{14}$$

Now we can rewrite Eq.(7) as

$$\begin{aligned}R=&\int_{V_S}\frac{S(P)}{\boldsymbol{\Sigma}_t(\boldsymbol{r},E)}\tilde{\xi}^+(P)dP\\ &+\int_{V_S}\tilde{\xi}^+(P)\iint C(\boldsymbol{r},E'\rightarrow E,\boldsymbol{\Omega}'\rightarrow\boldsymbol{\Omega})\psi(\boldsymbol{r},E',\boldsymbol{\Omega}')dE'd\Omega'dP\end{aligned} \tag{15}$$

The problem for coupling of two Monte Carlo calculations is to get in both calculations samples of particle events with exactly the same space, energy and direction variables. In general, this will never happen. For the midway method with coupling at a surface, this is solved by using a discretization of space, energy and direction at the coupling surface and assuming that surface crossing events within a certain discretized range have the same value of position, energy and direction.
Another way to solve the problem is using a next-event estimator that will force one or more of the particle variables to have a certain value. Looking at the last term of Eq.(15) we may have at a certain stage of the adjoint Monte Carlo simulation an adjoint particle leaving a collision or the adjoint source at $P_a=(\boldsymbol{r}_a,E_a,\boldsymbol{\Omega}_a)$, hence a sample of $\tilde{\xi}^+(P)$. In the forward Monte Carlo simulation we may have a collision

at $P_f=(\boldsymbol{r}_f,E_f,\boldsymbol{\Omega}_f)$, hence a sample of $\psi(\boldsymbol{r},E',\boldsymbol{\Omega}')$. By normal sampling of the collision kernel C we will never arrive at energy after collision equal to E_a, nor direction after collision $\boldsymbol{\Omega}_a$ as required for the product with $\tilde{\xi}^+(P)$. We can use the kernel $C(\boldsymbol{r},E_f\rightarrow E_a,\boldsymbol{\Omega}_f\rightarrow\boldsymbol{\Omega}_a)$ to calculate the probability that the energy after collision is E_a and the direction after collision is $\boldsymbol{\Omega}_a$. Obviously, the position of the forward and adjoint collision will not match. Therefore, we also apply a next-event estimator for the estimation of $\tilde{\xi}^+$ in Eq.(15) by including an additional step using the adjoint emission density according to Eq.(13):

$$\begin{aligned} R = &\int_{V_S}\frac{S(P)}{\boldsymbol{\Sigma}_t(\boldsymbol{r},E)}\int T^+(\boldsymbol{r}'\rightarrow\boldsymbol{r},E,\boldsymbol{\Omega})\tilde{\xi}^+(\boldsymbol{r}',E,\boldsymbol{\Omega})dV'dP \\ &+\int_{V_S}\frac{1}{\boldsymbol{\Sigma}_t(\boldsymbol{r},E)}\int T^+(\boldsymbol{r}'\rightarrow\boldsymbol{r},E,\boldsymbol{\Omega})\tilde{\xi}^+(\boldsymbol{r}',E,\boldsymbol{\Omega})dV' \\ &\text{x}\iint C(\boldsymbol{r},E'\rightarrow E,\boldsymbol{\Omega}'\rightarrow\boldsymbol{\Omega})\psi(\boldsymbol{r},E',\boldsymbol{\Omega}')dE'd\Omega'dP \end{aligned} \tag{16}$$

The kernel T^+ can be used to calculate the probability to have the next adjoint collision at $\boldsymbol{r}_f$. As the next collision site must be in the direction $\boldsymbol{\Omega}_a$ seen from $\boldsymbol{r}_a$, this probability will normally be zero. Therefore, we include also an adjoint scattering event in the formulation using Eq.(14). This leads to four terms as follows

$$R = R_1 + R_2 + R_3 + R_4 \tag{17}$$

with

$$R_1 = \int_{V_S}\frac{S(P)}{\boldsymbol{\Sigma}_t(\boldsymbol{r},E)}\int_{V_D} T^+(\boldsymbol{r}'\rightarrow\boldsymbol{r},E,\boldsymbol{\Omega})D(\boldsymbol{r}',E,\boldsymbol{\Omega})dV'dP \tag{18}$$

$$\begin{aligned} R_2 = &\int_{V_S}\frac{1}{\Sigma_t(\boldsymbol{r},E)}\int_{V_D} T^+(\boldsymbol{r}'\rightarrow\boldsymbol{r},E,\Omega)D(\boldsymbol{r}',E,\Omega)dV' \\ &\text{x}\iint C(\boldsymbol{r},E'\rightarrow E,\Omega'\rightarrow\Omega)\psi(\boldsymbol{r},E',\Omega')dE'd\Omega'dP \end{aligned} \tag{19}$$

$$\begin{aligned} R_3 = &\int_{V_S}\frac{S(P)}{\Sigma_t(\boldsymbol{r},E)}\int_{V_D} T^+(\boldsymbol{r}'\rightarrow\boldsymbol{r},E,\Omega) \\ &\text{x}\iint P^+(\boldsymbol{r}',E')C^+(\boldsymbol{r}',E'\rightarrow E,\Omega'\rightarrow\Omega)\tilde{\xi}^+(\boldsymbol{r}',E',\Omega')dE'd\Omega'dV'dP \end{aligned} \tag{20}$$

$$\begin{aligned} R_4 = &\int_{V_S}\frac{1}{\Sigma_t(\boldsymbol{r},E)}\int_{V_D} T^+(\boldsymbol{r}'\rightarrow\boldsymbol{r},E,\Omega) \\ &\text{x}\iint P^+(\boldsymbol{r}',E'')C^+(\boldsymbol{r}',E''\rightarrow E,\Omega''\rightarrow\Omega)\tilde{\xi}^+(\boldsymbol{r}',E'',\Omega'')dE''d\Omega''dV' \\ &\text{x}\iint C(\boldsymbol{r},E'\rightarrow E,\Omega'\rightarrow\Omega)\psi(\boldsymbol{r},E',\Omega')dE'd\Omega'dP \end{aligned} \tag{21}$$

Note that due to the perturbation in the adjoint calculation we have a complete separation in space for the collision sites of the forward particles, which must only be in volume V_S, and the collision sites for the adjoint particles, which must only be in volume V_D. Also note that although there are no adjoint scattering reactions in V_S, the adjoint collision density $\tilde{\xi}^+$ is not zero in V_S, as this volume is not a black absorber but a pure absorber for the adjoint particles with a finite absorption cross section. The first three terms R_1, R_2 and R_3 can now be estimated.

For R_1 we need a sample of a source position $\boldsymbol{r}_s$ from S and a detector position $\boldsymbol{r}_d$ and energy E from D (Fig. 2a). We can then calculate the probability of selecting the direction $\boldsymbol{\Omega}=(\boldsymbol{r}_d-\boldsymbol{r}_s)/|\boldsymbol{r}_d-\boldsymbol{r}_s|$, from D and the

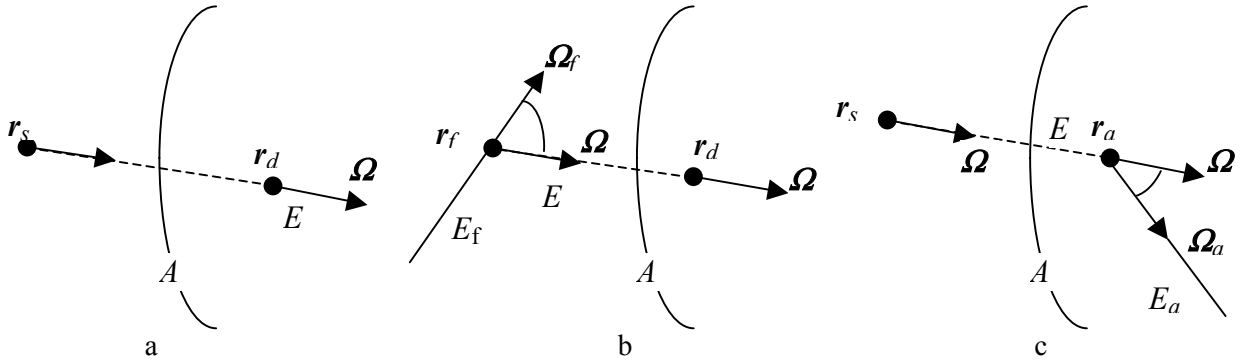

Fig. 2. Coupling of (a) a source and detector site; (b) a forward collision site and a detector site; (c) a source site and an adjoint collision site

probability for selecting the same direction $\boldsymbol{\Omega}$ as well as the energy E from S and finally calculate the probability $T^+(\boldsymbol{r}_d \rightarrow \boldsymbol{r}_s, E, \boldsymbol{\Omega})$. The product of all these probability gives the appropriate score. It will be clear that this term can only contribute if there is a certain range of overlap for the energy dependence of the source S and the detector sensitivity D.

For R_2 we need a sample of the forward collision density ψ, say at $(\boldsymbol{r}_f, E_f, \boldsymbol{\Omega}_f)$, and a sample of a detector position $\boldsymbol{r}_d$ from D (Fig. 2b). We can now calculate from the collision kernel C the probability of having a direction $\boldsymbol{\Omega}=(\boldsymbol{r}_d-\boldsymbol{r}_f)/|\boldsymbol{r}_d-\boldsymbol{r}_f|$. This will determine the energy E after collision. Then we can calculate the probability of selecting that direction $\boldsymbol{\Omega}$ and energy E from D. Again the product of these probabilities gives the required score. Whether this score is non-zero depends on the energy E and the sensitive energy range of D.

For R_3 we need a source position sample $\boldsymbol{r}_s$ from S and a sample of the adjoint collision density $\tilde{\xi}^+$, say at $(\boldsymbol{r}_a, E_a, \boldsymbol{\Omega}_a)$, (Fig. 2c). We can now calculate from the adjoint collision kernel C^+ the probability for having an adjoint collision with direction after collision equal to $\boldsymbol{\Omega}=(\boldsymbol{r}_a-\boldsymbol{r}_s)/|\boldsymbol{r}_a-\boldsymbol{r}_s|$, applying a weight factor P^+ and calculating the probability from the adjoint transport kernel T^+ for having the next adjoint collision at $\boldsymbol{r}_s$. This scattering angle of the adjoint collision will determine the energy E after collision. Then we can calculate the probability of selecting that energy E and the direction $\boldsymbol{\Omega}$ from D. Again the product of these probabilities gives the required score. Whether this score is non-zero depends on the energy E and the energy range of the source S.

The simulation of R_4 can be imagined as follows. Given a sample of the forward collision density ψ at $(\boldsymbol{r}_f, E_f, \boldsymbol{\Omega}_f)$ and a sample of the adjoint collision density $\tilde{\xi}^+$ at $(\boldsymbol{r}_a, E_a, \boldsymbol{\Omega}_a)$ (see Fig. 3) we can easily match the direction and position by calculating the probability from the adjoint collision kernel C^+ for having an

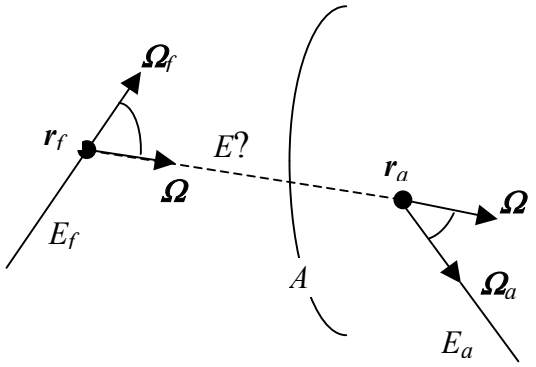

Fig. 3. Coupling of a forward and an adjoint collision point

adjoint collision with direction after collision equal to $\Omega=(r_a-r_f)/|r_a-r_f|$, applying a weight factor P^+ and calculating the probability from the adjoint transport kernel T^+ for having the next adjoint collision at r_f. For the forward collision we can calculate the probability for a direction after scattering equal to Ω from the collision kernel C. The energy after collision is also fixed together with the direction after scattering, both for the forward and the adjoint collision. In the case of a multigroup treatment, there is a chance that the energy group numbers after the forward and the adjoint collision match, resulting in a non-zero score. This is the basis of the next-event estimator of Ueki et al.[2]. However, for the continuous energy case, the energies after scattering of the forward and adjoint collision will not be equal and this next-event estimator will not work.

Therefore, a further step to be taken is the inclusion of one more transport step of the adjoint particle according to Eq.(13) in Eq.(21), leading to

$$R_4 = \int_{V_S} \frac{1}{\Sigma_t(\boldsymbol{r},E)} \int_{V_D} T^+(\boldsymbol{r}' \to \boldsymbol{r}, E, \boldsymbol{\Omega}) \iint P^+(\boldsymbol{r}', E'') C^+(\boldsymbol{r}', E'' \to E, \boldsymbol{\Omega}'' \to \boldsymbol{\Omega})$$
$$\text{x} \int_{V_D} T^+(\boldsymbol{r}'' \to \boldsymbol{r}', E'', \boldsymbol{\Omega}'') \xi^+(\boldsymbol{r}'', E'', \boldsymbol{\Omega}'') dV'' dE'' d\boldsymbol{\Omega}'' dV' \qquad (22)$$
$$\text{x} \iint C(\boldsymbol{r}, E' \to E, \boldsymbol{\Omega}' \to \boldsymbol{\Omega}) \psi(\boldsymbol{r}, E', \boldsymbol{\Omega}') dE' d\boldsymbol{\Omega}' dP$$

The Monte Carlo sampling of Eq.(22) goes as follows. Given a sample of the forward collision density ψ at (r_f,E_f,Ω_f) and a sample of the adjoint emission density ξ^+ at (r_a,E_a,Ω_a) (see Fig. 4) we can try to find a next adjoint collision site r along the line $r=r_a-s\Omega_a$ such that after an adjoint collision at r with direction after scattering equal to $\Omega=(r-r_f)/|r-r_f|$, and a forward collision at r_f with the same direction Ω after scattering the energies of the forward and the adjoint particle after scattering are equal. A further condition is that point r lies in the volume V_D. There is no guarantee that such a point r exists. For instance, if $E_a>E_f$ no such point exists, as the adjoint particle will gain energy in a collision and the forward particle will lose energy in a collision and the energies after collision cannot be equal. Nonetheless, in the situation of Fig. 4 one can see that if the distance s travelled by the adjoint particle increases, the cosine of the scattering angle to direction Ω increases and hence the energy after the adjoint collision. On the other hand, with increasing s the cosine of the scattering angle of the forward collision first decreases (until $\Omega=\Omega_f$) and the energy E after collision decreases to E_f for an elastic collision and increases again until $\Omega=-\Omega_a$ when s going to infinity (provided point r is still within V_D). For other positions r_f and r_a and directions Ω_f and

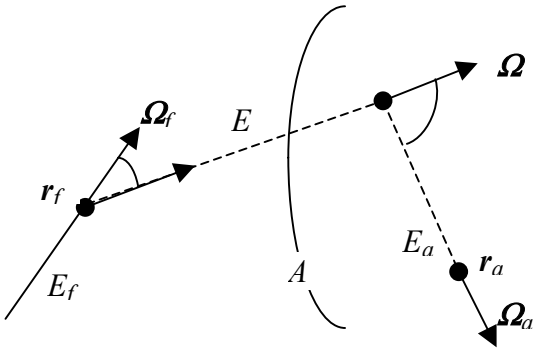

Fig. 4. Coupling of a forward collision site and an adjoint emission site

$\boldsymbol{\Omega}_a$ the variation of the energies after collision may be different, but depending on the values of all particle variables a suitable adjoint collision point $\boldsymbol{r}$ may be found.

We now evaluate the score for such an event. In words, we need to calculate the probability $T^+(\boldsymbol{r}_a \rightarrow \boldsymbol{r}, E_a, \boldsymbol{\Omega}_a)$ for having the next adjoint collision site at $\boldsymbol{r}$, the probability $C^+(\boldsymbol{r}, E_a \rightarrow E, \boldsymbol{\Omega}_a \rightarrow \boldsymbol{\Omega})$ times the adjoint weight factor $P^+(\boldsymbol{r}, E_a)$, the probability $T^+(\boldsymbol{r} \rightarrow \boldsymbol{r}_f, E, \boldsymbol{\Omega})$ for a new adjoint collision site at $\boldsymbol{r}_f$ and the probability $C(\boldsymbol{r}_f, E_f \rightarrow E, \boldsymbol{\Omega}_f \rightarrow \boldsymbol{\Omega})$ for having a forward collision with direction after scattering equal to $\boldsymbol{\Omega}$.

Up to now, we formulated the score at a successful coupling of two sites as the product of a number of probabilities. However, this was a somewhat loose formulation. The numerical application of the next-event estimators indicated above for the various terms of R require a more precise evaluation as the various kernels for transport and collision contain δ-functions. The adjoint transport kernel T^+ is equal to the normal forward transport kernel, except that the adjoint particle moves into the direction opposite to $\boldsymbol{\Omega}$ [4]

$$T^+(\boldsymbol{r}' \rightarrow \boldsymbol{r}, E, \boldsymbol{\Omega}) = \boldsymbol{\Sigma}_t(\boldsymbol{r}, E) \exp\left\{ -\int_0^{|r-r'|} \boldsymbol{\Sigma}_t(\boldsymbol{r} + s\boldsymbol{\Omega}, E) ds \right\} \delta\left(\boldsymbol{\Omega} + \frac{\boldsymbol{r} - \boldsymbol{r}'}{|\boldsymbol{r} - \boldsymbol{r}'|} \right) \Big/ |\boldsymbol{r} - \boldsymbol{r}'|^2 . \qquad (23)$$

The exponential term represents the attenuation with in the exponent the number of mean free paths travelled from $\boldsymbol{r}$' to $\boldsymbol{r}$. The δ-function forces the movement of the particle into the direction -$\boldsymbol{\Omega}$. The collision kernel is normally a summation of scattering kernels for the various nuclides and reaction types at a certain position in the system. For simplicity we restrict our derivation here to a single nuclide and reaction type. As the energy after scattering is normally determined by the cosine of the scattering angle $\boldsymbol{\Omega}' \cdot \boldsymbol{\Omega}$ and the energy before the collision (neutron elastic and inelastic discrete level scattering; Compton scattering of photons) we write for the collision kernel

$$\begin{aligned} C(\boldsymbol{r}, E' \rightarrow E, \boldsymbol{\Omega}' \rightarrow \boldsymbol{\Omega}) &= \frac{\boldsymbol{\Sigma}_s(\boldsymbol{r}, E', \boldsymbol{\Omega}' \rightarrow \boldsymbol{\Omega})}{\boldsymbol{\Sigma}_t(\boldsymbol{r}, E')} \delta\left(E - E_s(E', \boldsymbol{\Omega}' \cdot \boldsymbol{\Omega})\right) \\ &= \frac{\boldsymbol{\Sigma}_s(\boldsymbol{r}, E')}{\boldsymbol{\Sigma}_t(\boldsymbol{r}, E')} f(E', \boldsymbol{\Omega}' \cdot \boldsymbol{\Omega}) \delta\left(E - E_s(E', \boldsymbol{\Omega}' \cdot \boldsymbol{\Omega})\right) \end{aligned} \qquad (24)$$

with E_s the energy after scattering as a function of E' and $\boldsymbol{\Omega}' \cdot \boldsymbol{\Omega}$ and $f(\boldsymbol{\Omega}' \cdot \boldsymbol{\Omega})$ the angular scattering probability. The adjoint collision kernel is given by

$$C^+(\boldsymbol{r},E'\to E,\boldsymbol{\Omega}'\to\boldsymbol{\Omega})=\frac{\boldsymbol{\Sigma}_s(\boldsymbol{r},E,\boldsymbol{\Omega}\to\boldsymbol{\Omega}')}{\boldsymbol{\Sigma}^+(\boldsymbol{r},E')}\delta\left(E'-E_s(E,\boldsymbol{\Omega}\cdot\boldsymbol{\Omega}')\right)$$
$$=\frac{\boldsymbol{\Sigma}_s(\boldsymbol{r},E)}{\boldsymbol{\Sigma}^+(\boldsymbol{r},E')}f(E,\boldsymbol{\Omega}\cdot\boldsymbol{\Omega}')\delta\left(E'-E_s(E,\boldsymbol{\Omega}\cdot\boldsymbol{\Omega}')\right) \tag{25}$$

with the so-called adjoint cross section Σ^+ given by [4]

$$\boldsymbol{\Sigma}^+(\boldsymbol{r},E')=\iint\boldsymbol{\Sigma}_s(\boldsymbol{r},E\to E',\boldsymbol{\Omega}\to\boldsymbol{\Omega}')dEd\boldsymbol{\Omega} \tag{26}$$

and the adjoint weight factor by

$$P^+(\boldsymbol{r},E')=\frac{\boldsymbol{\Sigma}^+(\boldsymbol{r},E')}{\boldsymbol{\Sigma}_t(\boldsymbol{r},E')} \tag{27}$$

For the first contribution R_1 of Eq.(18) to the detector response R with coupling of a source and detector site we start with a sample of a source position $\boldsymbol{r}_S$ from S with a particle weight w_S and a detector position $\boldsymbol{r}_d$ and energy E from D with a particle weight w_d. This means that the integration over these variables required in Eq.(18) will be performed with the Monte Carlo method, i.e. by repeated sampling and averaging the final scores. What rests is the integration over $\boldsymbol{\Omega}$ which must be performed analytically, taking into account the δ-function in T^+. Hence the estimator $\hat{R}_1$ for the first term becomes

$$\hat{R}_1=w_sw_d\int_{4\pi}\frac{S(\boldsymbol{r}_s,E,\boldsymbol{\Omega})}{\int S(\boldsymbol{r}_s,E',\boldsymbol{\Omega}')dE'd\Omega'}\frac{1}{\boldsymbol{\Sigma}_t(\boldsymbol{r}_s,E)}T^+(\boldsymbol{r}_d\to\boldsymbol{r}_s,E,\boldsymbol{\Omega})\frac{D(\boldsymbol{r}_d,E,\boldsymbol{\Omega})}{\int D(\boldsymbol{r}_d,E,\boldsymbol{\Omega}')d\Omega'}d\Omega$$
$$=w_sw_d\frac{S(\boldsymbol{r}_s,E,\boldsymbol{\Omega})}{\int S(\boldsymbol{r}_s,E',\boldsymbol{\Omega}')dE'd\Omega'}\frac{e^{-z(\boldsymbol{r}_d,\boldsymbol{r}_s,E)}}{|\boldsymbol{r}_d-\boldsymbol{r}_s|^2}\frac{D(\boldsymbol{r}_d,E,\boldsymbol{\Omega})}{\int D(\boldsymbol{r}_d,E,\boldsymbol{\Omega}')d\Omega'} \tag{28}$$

with in the last term $\boldsymbol{\Omega}$ equal to $(\boldsymbol{r}_d-\boldsymbol{r}_S)/|\boldsymbol{r}_d-\boldsymbol{r}_S|$ and $z(\boldsymbol{r}_d,\boldsymbol{r}_S)$ the number of mean free path between $\boldsymbol{r}_d$ and $\boldsymbol{r}_S$ at energy E.

For the contribution R_2 of Eq.(19) with coupling of a collision site and a detector site we start with a sample of the collision density ψ at $(\boldsymbol{r}_f,E_f,\boldsymbol{\Omega}_f)$ with a particle weight w_S and a sample of a detector position $\boldsymbol{r}_d$ from D with a particle weight w_d . Then for the estimator $\hat{R}_2$ we have to evaluate analytically the integrals over E and $\boldsymbol{\Omega}$.

$$\hat{R}_2=w_fw_d\iint\frac{1}{\boldsymbol{\Sigma}_t(\boldsymbol{r}_f,E)}T^+(\boldsymbol{r}_d\to\boldsymbol{r}_f,E,\boldsymbol{\Omega})\frac{D(\boldsymbol{r}_d,E,\boldsymbol{\Omega})}{\iint D(\boldsymbol{r}_d,E',\boldsymbol{\Omega}')dE'd\Omega'}C(\boldsymbol{r}_f,E_f\to E,\boldsymbol{\Omega}_f\to\boldsymbol{\Omega})dEd\Omega$$
$$=w_fw_d\frac{e^{-z(\boldsymbol{r}_d,\boldsymbol{r}_f,E)}}{|\boldsymbol{r}_f-\boldsymbol{r}_d|^2}\frac{D(\boldsymbol{r}_d,E,\boldsymbol{\Omega})}{\int D(\boldsymbol{r}_d,E',\boldsymbol{\Omega}')dE'd\Omega'}\frac{\boldsymbol{\Sigma}_s(\boldsymbol{r}_f,E_f)}{\boldsymbol{\Sigma}_t(\boldsymbol{r}_f,E_f)}f(E_f,\boldsymbol{\Omega}_f\cdot\boldsymbol{\Omega}) \tag{29}$$

with in the last term $\boldsymbol{\Omega}$ equal to $(\boldsymbol{r}_d-\boldsymbol{r}_f)/|\boldsymbol{r}_d-\boldsymbol{r}_f|$ and $E=E_s(E_f,\boldsymbol{\Omega}_f.\boldsymbol{\Omega})$.

For the third contribution R_3 of Eq.(20) with coupling of a source site and an adjoint collision site we start with a sample of a source position $\boldsymbol{r}_s$ from S with a particle weight w_s and a sample of the adjoint collision density ξ^+ at ($\boldsymbol{r}_a$,E_a,$\boldsymbol{\Omega}_a$) with a particle weight w_a. Then for the estimator R_3 we have to evaluate analytically the integrals over E and $\boldsymbol{\Omega}$.

$$\begin{aligned} R_3 &= w_s w_a \iint \frac{S(\boldsymbol{r}_s, E, \boldsymbol{\Omega})}{\iint S(\boldsymbol{r}_s, E', \boldsymbol{\Omega}') dE' d\Omega'} \frac{1}{\boldsymbol{\Sigma}_t(\boldsymbol{r}_s, E)} T^+(\boldsymbol{r}_a \to \boldsymbol{r}_s, E, \boldsymbol{\Omega}) \\ &\quad \text{x } P^+(\boldsymbol{r}_a, E_a) C^+(\boldsymbol{r}_a, E_a \to E, \boldsymbol{\Omega}_a \to \boldsymbol{\Omega}) dE d\Omega \\ &= w_s w_a \frac{S(\boldsymbol{r}_s, E, \boldsymbol{\Omega})}{\iint S(\boldsymbol{r}_s, E', \boldsymbol{\Omega}') dE' d\Omega'} \frac{e^{-z(\boldsymbol{r}_a, \boldsymbol{r}_s, E)}}{|\boldsymbol{r}_s - \boldsymbol{r}_a|^2} \frac{\boldsymbol{\Sigma}_s(\boldsymbol{r}_a, E)}{\boldsymbol{\Sigma}_t(\boldsymbol{r}_a, E_a)} f(E, \boldsymbol{\Omega}_a \cdot \boldsymbol{\Omega}) \Bigg/ \left| \frac{dE_s(E, \boldsymbol{\Omega}_a \cdot \boldsymbol{\Omega})}{dE} \right| \end{aligned} \tag{30}$$

Finally, for estimating R_4 according to Eq.(22) we need a sample of the forward collision density ψ, say at ($\boldsymbol{r}_f$,E_f,$\boldsymbol{\Omega}_f$), with statistical weight w_f and a sample of the adjoint collision density ξ^+, say at ($\boldsymbol{r}_a$,E_a,$\boldsymbol{\Omega}_a$), with statistical weight w_a. Then for the estimator R_4 we have to evaluate analytically the integrals over $\boldsymbol{r}$, E and $\boldsymbol{\Omega}$.

$$\begin{aligned} R_4 = w_f w_a \int_{V_D} \iint \frac{1}{\boldsymbol{\Sigma}_t(\boldsymbol{r}_f, E)} & T^+(\boldsymbol{r} \to \boldsymbol{r}_f, E, \boldsymbol{\Omega}) P^+(\boldsymbol{r}, E_a) C^+(\boldsymbol{r}, E_a \to E, \boldsymbol{\Omega}_a \to \boldsymbol{\Omega}) \\ & \text{x} T^+(\boldsymbol{r}_a \to \boldsymbol{r}, E_a, \boldsymbol{\Omega}_a) C(\boldsymbol{r}_f, E_f \to E, \boldsymbol{\Omega}_f \to \boldsymbol{\Omega}) dV dE d\Omega \end{aligned} \tag{31}$$

As the integrand of Eq.(31) contains 4 δ-functions (2 times from T^+, from C^+ and from C) and we only have three integration variables it looks like that this estimator won't work. However, we can substitute for the volume integration $\boldsymbol{r}=\boldsymbol{r}_a+s\boldsymbol{\Omega}^*$ with $s=|\boldsymbol{r}-\boldsymbol{r}_a|$ the path length travelled from $\boldsymbol{r}_a$ and $\boldsymbol{\Omega}^*$ a unit direction vector. Then $dV=s^2 ds d\boldsymbol{\Omega}^*$ and we can carry out easily the integrations over $\boldsymbol{\Omega}$, $\boldsymbol{\Omega}^*$ and E. The δ-function from the second adjoint transport kernel becomes

$$\delta\left(\boldsymbol{\Omega}_a + \frac{\boldsymbol{r} - \boldsymbol{r}_a}{|\boldsymbol{r} - \boldsymbol{r}_a|} \right) = \delta\left(\boldsymbol{\Omega}_a + \boldsymbol{\Omega}^* \right) \tag{32}$$

and after integration over $\boldsymbol{\Omega}^*$ gives $\boldsymbol{\Omega}^*=-\boldsymbol{\Omega}_a$ and $\boldsymbol{r}=\boldsymbol{r}_a - s\boldsymbol{\Omega}_a$. The δ-function from the first adjoint transport kernel becomes

$$\delta\left(\boldsymbol{\Omega} + \frac{\boldsymbol{r}_f - \boldsymbol{r}_a + s\boldsymbol{\Omega}_a}{|\boldsymbol{r}_f - \boldsymbol{r}_a + s\boldsymbol{\Omega}_a|} \right) \tag{33}$$

which determines $\boldsymbol{\Omega}$ as a function of s. The δ-function from the forward scattering kernel C fixes the energy E as $E_s(E_f, \boldsymbol{\Omega}_f, \boldsymbol{\Omega})$ with implicit dependence on s via $\boldsymbol{\Omega}$. We now have

$$R_4 = w_f w_a \int_{\boldsymbol{r}\in V_D} \frac{\mathrm{e}^{-z(\boldsymbol{r},\boldsymbol{r}_f,E)}}{|\boldsymbol{r}_f-\boldsymbol{r}|^2}\boldsymbol{\Sigma}_s(\boldsymbol{r},E_a) f(E,\boldsymbol{\Omega}_a\cdot\boldsymbol{\Omega})\delta\left(E_a - E_s(E,\boldsymbol{\Omega}_f\cdot\boldsymbol{\Omega})\right) \\ \mathrm{x}\,\mathrm{e}^{-z(\boldsymbol{r}_a,\boldsymbol{r},E_a)}\frac{\boldsymbol{\Sigma}_s(\boldsymbol{r}_f,E_f)}{\boldsymbol{\Sigma}_t(\boldsymbol{r}_f,E_f)} f(E_f,\boldsymbol{\Omega}_f\cdot\boldsymbol{\Omega})ds \tag{34}$$

Integration of the δ-function from the adjoint scattering kernel C^+ over s can now be written as

$$\int \delta\left(E_a - E_s(E_a,\boldsymbol{\Omega}_a\cdot\boldsymbol{\Omega})\right)ds = \int \delta\left(E_a - E_s(E_a,\boldsymbol{\Omega}_a\cdot\boldsymbol{\Omega})\right)\frac{ds}{dE_s}dE_s = \frac{1}{\left(\frac{dE_s(E,\boldsymbol{\Omega}_a\cdot\boldsymbol{\Omega})}{ds}\right)_{E=E_s^{-1}(E_a,\boldsymbol{\Omega}_a\cdot\boldsymbol{\Omega})}} \tag{35}$$

and

$$R_4 = w_f w_a \frac{\mathrm{e}^{-z(\boldsymbol{r},\boldsymbol{r}_f,E)}}{|\boldsymbol{r}_\mathrm{f}-\boldsymbol{r}|^2}\boldsymbol{\Sigma}_s(\boldsymbol{r},E) f(E,\boldsymbol{\Omega}_a\cdot\boldsymbol{\Omega})\mathrm{e}^{-z(\boldsymbol{r}_a,\boldsymbol{r},E_a)} \\ \mathrm{x}\,\frac{\boldsymbol{\Sigma}_s(\boldsymbol{r}_f,E_f)}{\boldsymbol{\Sigma}_t(\boldsymbol{r}_f,E_f)} f(E_f,\boldsymbol{\Omega}_f\cdot\boldsymbol{\Omega})\Bigg/\left(\frac{dE_s(E,\boldsymbol{\Omega}_a\cdot\boldsymbol{\Omega}}{ds}\right)_{E=E_s^{-1}(E_a,\boldsymbol{\Omega}_a\cdot\boldsymbol{\Omega})} \tag{36}$$

with the condition for s

$$E_a = E_s(E,\boldsymbol{\Omega}_a\cdot\boldsymbol{\Omega}) = E_s(E_s(E_f,\mu_{0f}),\mu_{0a}) \tag{37}$$

with $\mu_{oa}=\boldsymbol{\Omega}_a\cdot\boldsymbol{\Omega}$ and $\mu_{of}=\boldsymbol{\Omega}_f\cdot\boldsymbol{\Omega}$ the cosines of the scattering angles in the laboratory system for the scatterings at $\boldsymbol{r}$ and $\boldsymbol{r}_f$, respectively, both depending on s.
For elastic neutron scattering with energy before scattering equal to E_f and energy after scattering equal to E we have [5]

$$E = E_f\frac{A^2+2A\mu_{cf}+1}{(A+1)^2} \tag{38}$$

with μ_{cf} the cosine of the scattering angle in the centre-of-mass system and A the atom mass relative to the neutron mass. Likewise with energy before scattering equal to E and energy after scattering equal to E_a and thus for an adjoint collision with energy before scattering equal to E_a and energy after scattering equal to E

$$E_a = E\frac{A^2+2A\mu_{ca}+1}{(A+1)^2} \tag{39}$$

Hence, the implicit condition for s is

$$E_a = E_f \frac{A^2 + 2A\mu_{cf}(s) + 1}{(A+1)^2} \frac{A^2 + 2A\mu_{ca}(s) + 1}{(A+1)^2} \tag{40}$$

For elastic neutron scattering the cosine of the scattering angle in the laboratory system μ_o is related to that in the centre-of-mass system μ_c by

$$\mu_0 = \frac{A\mu_c + 1}{\sqrt{A^2 + 2A\mu_c + 1}} \tag{41}$$

Its derivative with respect to μ_c is

$$\frac{d\mu_0}{d\mu_c} = \frac{A^2(A + \mu_c)}{\left(A^2 + 2A\mu_c + 1\right)^{3/2}} \tag{42}$$

To calculate the derivative in Eq.(36) we have to realise that the energy E after the adjoint collision is related to s via μ_{oa} and $\boldsymbol{\Omega}$ related to s via the δ-function of expression (33). Hence we have

$$\frac{dE_s}{ds} = \frac{\partial E_s}{\partial E}\frac{dE}{ds} + \frac{\partial E_s}{\partial \mu_{0a}}\frac{d\mu_{0a}}{ds} = \frac{\partial E_s}{\partial E}\frac{dE}{d\mu_{cf}}\frac{d\mu_{cf}}{d\mu_{0f}}\frac{d\mu_{0f}}{ds} + \frac{\partial E_s}{\partial \mu_{ca}}\frac{d\mu_{ca}}{d\mu_{0a}}\frac{d\mu_{0a}}{ds} \tag{43}$$

For the calculation of the derivatives of μ_o with respect to s we see from Fig. 5 with $t=|\boldsymbol{r}-\boldsymbol{r}_f|=|\boldsymbol{r}_a-\boldsymbol{r}_f-s\boldsymbol{\Omega}_a|$ and $b=|\boldsymbol{r}_a-\boldsymbol{r}_f|$ that

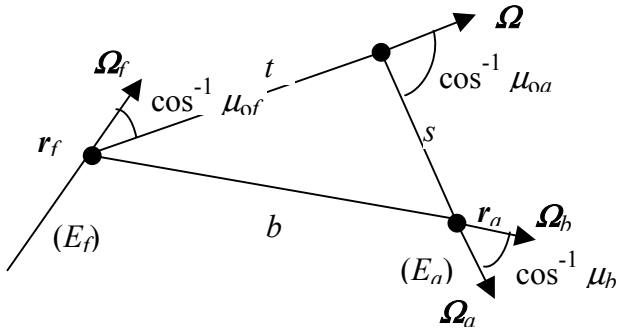

Fig. 5. Calculation of the derivatives $\dfrac{d\mu_0}{ds}$

$$t^2 = b^2 + s^2 - 2bs\mu_b \tag{44}$$

From which

$$2t\frac{dt}{ds} = 2s - 2b\mu_b \tag{45}$$

and

$$\frac{dt}{ds} = \frac{s - b\mu_b}{t} \tag{46}$$

Hence,

$$\frac{d\mu_{0a}}{ds} = \frac{d}{ds}\boldsymbol{\Omega}\cdot\boldsymbol{\Omega}_a = \frac{d}{ds}\frac{(\boldsymbol{r}_a-\boldsymbol{r}_f)\cdot\boldsymbol{\Omega}_a - s}{t} = \frac{-t-[(\boldsymbol{r}_a-\boldsymbol{r}_f)\cdot\boldsymbol{\Omega}_a - s]\dfrac{dt}{ds}}{t^2} = \frac{(s-b\mu_b)^2-t^2}{t^3} \tag{47}$$

with

$$\mu_b = \boldsymbol{\Omega}_b\cdot\boldsymbol{\Omega}_a = \frac{\boldsymbol{r}_a-\boldsymbol{r}_f}{|\,\boldsymbol{r}_a-\boldsymbol{r}_f\,|}\cdot\boldsymbol{\Omega}_a \tag{48}$$

Also

$$\begin{aligned}\frac{d\mu_{0f}}{ds} &= \frac{d}{ds}\boldsymbol{\Omega}\cdot\boldsymbol{\Omega}_f = \frac{d}{ds}\frac{(\boldsymbol{r}_a-\boldsymbol{r}_f)\cdot\boldsymbol{\Omega}_f - s\boldsymbol{\Omega}_a\cdot\boldsymbol{\Omega}_f}{t} \\ &= \frac{-t\mu_{af}-[(\boldsymbol{r}_a-\boldsymbol{r}_f)\cdot\boldsymbol{\Omega}_f - s\mu_{af}]\dfrac{dt}{ds}}{t^2} = \frac{(s-b\mu_b)(s\mu_{af}-b\mu_{bf})-t^2\mu_{af}}{t^3}\end{aligned} \tag{49}$$

with $\mu_{af}=\boldsymbol{\Omega}_a\cdot\boldsymbol{\Omega}_f$ and $\mu_{bf}=\boldsymbol{\Omega}_b\cdot\boldsymbol{\Omega}_f$.
From Eq.(43) we have

$$\frac{dE_s}{ds} = \frac{2A}{(A+1)^2}E_f\left[\frac{E_a}{E}\frac{1}{\dfrac{d\mu_{0f}}{d\mu_{cf}}}\frac{d\mu_{0f}}{ds} + \frac{E}{E_f}\frac{1}{\dfrac{d\mu_{0a}}{d\mu_{ca}}}\frac{d\mu_{0a}}{ds}\right] \tag{50}$$

With this result the estimator in Eq.(36) can be calculated.

We can summarize the procedure as follows. From a forward Monte Carlo calculation for the unperturbed system we register a number of source events and collision events. From the collision events we only need those that occur in volume V_S. From an adjoint Monte Carlo calculation for the perturbed system (i.e. we end an adjoint history if the adjoint particle crosses surface A) we register a number of adjoint emission events, i.e. adjoint particles emitted by the adjoint source (the detector) or at adjoint collisions. For all pairs of registered forward and adjoint events from one forward and one adjoint history we apply the appropriate estimator from R_1 to R_4, depending on the selected forward and adjoint event. The desired detector response is obtained as the average over the number of forward and adjoint histories of all those estimates.

3. NUMERICAL EXAMPLE

To demonstrate numerically the theory developed in Sect. 2 we adopted the system from Fig. 5, consisting of a cylinder of 12.5-cm radius and 26 cm long. A spherical neutron source of 1-cm radius emits neutrons with a uniform energy distribution between 13.5 and 14.5 MeV. The detector registers the neutron flux per unit energy for a number of energy ranges in a 1-cm sphere. The source and detector spheres are located symmetrically in the system with their centre points along the system axis and 6 cm apart. The system is homogeneously filled with an artificial nuclide with mass A=12, including the source and detector regions. A constant elastic scattering cross section of 0.8 cm^{-1} with isotropic scattering in the centre-of-mass system is assumed and a $1/v$ absorption cross section of 0.32 cm^{-1} at 1 MeV.

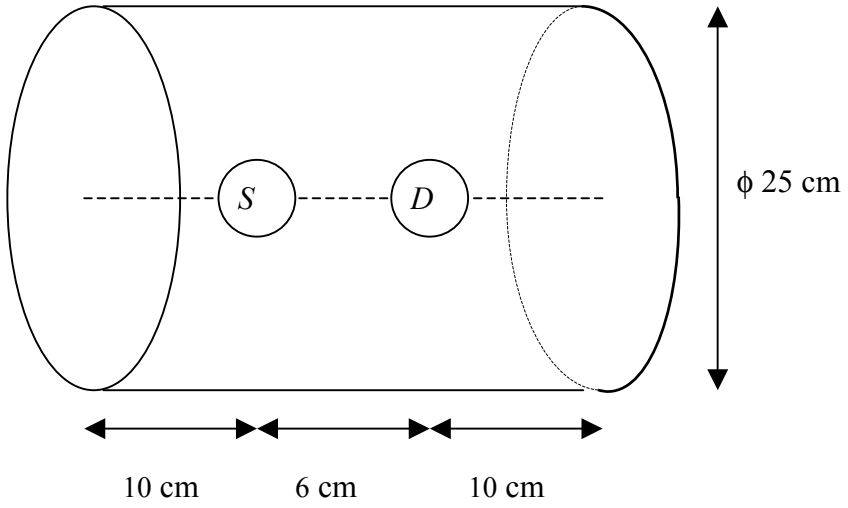

Fig. 5 Geometry of sample problem

For the forward calculation 10^7 neutrons were used and a collision estimator to obtain the detector response. For the adjoint calculation also 10^7 particle histories were used together with a collision estimator, but here a separate calculation has to be performed for each detector energy range. For the coupled calculation 10^6 particle histories were used both in the forward and the adjoint part.
Table I shows a fair agreement between the full forward, the full adjoint and the coupled forward-adjoint calculation, although some results of the coupled forward-adjoint calculation, especially for the lower energy ranges, seemed to be somewhat low. As the system is geometrically symmetric, there is no big difference in efficiency of the forward and adjoint calculation. However, the coupled calculation with 1/10 of the histories of the fully adjoint calculation results in much smaller standard deviations. For the coupled next-event estimator both forward and adjoint histories must be generated. In addition the computation of

Table I. Comparison of next-event coupling estimator with forward and adjoint calculations

	forward		adjoint		coupled forward-adjoint	
det. energy range (MeV)	flux ϕ ($cms^{-1}eV^{-1}$)	σ (%)	flux ϕ ($cms^{-1}eV^{-1}$)	σ (%)	flux ϕ ($cms^{-1}eV^{-1}$)	σ (%)
1 - 1.5	$3.72\ 10^{-10}$	1.5	$3.45\ 10^{-10}$	3.9	$3.28\ 10^{-10}$	1.2
1.5 – 2	$4.61\ 10^{-10}$	1.3	$4.46\ 10^{-10}$	2.9	$4.10\ 10^{-10}$	0.9
2 - 3	$5.10\ 10^{-10}$	1.0	$5.05\ 10^{-10}$	2.3	$4.59\ 10^{-10}$	0.9
3 - 4	$5.20\ 10^{-10}$	1.0	$5.00\ 10^{-10}$	1.9	$4.72\ 10^{-10}$	0.8
4 -5	$4.82\ 10^{-10}$	1.1	$4.55\ 10^{-10}$	1.8	$4.34\ 10^{-10}$	0.7
5 - 6	$4.25\ 10^{-10}$	1.2	$4.06\ 10^{-10}$	1.8	$3.90\ 10^{-10}$	0.8
6 - 7	$3.71\ 10^{-10}$	1.4	$3.47\ 10^{-10}$	2.0	$3.36\ 10^{-10}$	0.7
7 - 8	$3.04\ 10^{-10}$	1.6	$2.76\ 10^{-10}$	2.2	$2.89\ 10^{-10}$	0.9
8 - 9	$2.56\ 10^{-10}$	1.8	$2.35\ 10^{-10}$	2.3	$2.40\ 10^{-10}$	0.6
9 - 10	$2.01\ 10^{-10}$	2.1	$1.97\ 10^{-10}$	2.5	$1.95\ 10^{-10}$	0.7
10 - 11	$1.67\ 10^{-10}$	2.4	$1.58\ 10^{-10}$	2.8	$1.64\ 10^{-10}$	0.7
11 - 12	$1.29\ 10^{-10}$	2.8	$1.22\ 10^{-10}$	3.1	$1.29\ 10^{-10}$	0.6
12 - 13	$1.05\ 10^{-10}$	3.2	$9.62\ 10^{-11}$	3.5	$1.03\ 10^{-10}$	1.3
13 - 13.5	$8.30\ 10^{-11}$	5.0	$8.26\ 10^{-11}$	3.7	$8.07\ 10^{-11}$	0.6
13.5 - 14	$1.18\ 10^{-10}$	4.4	$1.15\ 10^{-10}$	3.3	$1.12\ 10^{-10}$	0.4
14 - 14.5	$7.84\ 10^{-11}$	5.4	$7.94\ 10^{-11}$	3.8	$7.44\ 10^{-11}$	0.4

a possible coupled score, especially for the estimator of R_4, takes appreciable computer time to find the intermediate scattering site and the more if the number of collisions per history increases. Nonetheless, the overall computer time for the coupled calculation with 10^6 histories is comparable with the time for the fully adjoint calculation with 10^7 particle histories, except for the low energy ranges, where the computer time of the coupling methods increases significantly as more collision sites are generated and the number of coupling possibilities to be considered increases quadratically. Nonetheless the coupling methods remains by far more efficient.

4. DISCUSSION AND CONCLUSIONS

We can conclude that the theory for coupling of forward and adjoint Monte Carlo calculations with a next-event estimator as derived in Sect. 2 is valid and can be implemented in a computer program to get numerical results. Although the theory looks complicated and the derivation of the next-event estimators require a careful analysis, the basic principle can be readily understood when visualising the various situations that occur when coupling forward and adjoint sites as shown in Fig. 2 and 4.

In this paper the theory and practice of an adjoint Monte Carlo calculation with continuous energy is assumed to be known. In fact, this theory leaves open some variation, especially with regard to a general transformation of the adjoint transport equation with respect to energy, which is important for neutron transport[4]. In order not to complicate the theory and formulae further, we did not include that transformation or biasing of the adjoint transport equation with a factor $1/E$ in the derivation in Sect. 2, but it was actually used in the numerical calculation.

Some other aspects should be discussed. In the theory developed here and the numerical example, only elastic scattering was assumed. For inelastic discrete level scattering the relations between the scattering angles in the laboratory system and the centre-of-mass system as well as the energy after scattering as a function of the scattering angle also involve the level energy of the inelastic scattering and the derivatives needed in Eq.(43) change. As the structure of these relations remain the same, the case of inelasic discrete level scattering can easily be included.

If the scattering material allows for more than one scattering reaction (e.g. elastic scattering and various levels of inelastic scattering) the forward and adjoint collision kernels will be composed of a summation over all scattering reaction types. There may also be a mixture of various nuclides in different zones of the system. In that case it is possible to include the summation in the estimator. Another possibility is to select one nuclide and reaction type in a Monte Carlo sense and apply the estimator as in the theory developed here.

There may also be reaction types like continuous inelastic scattering or $(n,2n)$-reactions for which there is no unique relation between the energy after scattering and the scattering angle. In that case one does not need to apply the estimator of Eq.(36) for R_4 with an intermediate scattering site, as it will in general be possible to match the energies of the forward and adjoint particle in the situation of Fig. 3.

In the example of Sect. 3 we coupled only the collision sites from one forward history with the adjoint collision sites of one adjoint history. However, there is no restriction to consider only pairs of collision sites from one history. In fact one can couple any forward collision site from any forward history to any adjoint collision site from any adjoint history. It will be clear that considering all possible combinations of collision sites that have been sampled during the complete forward and adjoint calculations will require a huge amount of computer time if the number of histories is large. Ueki et al.[2] demonstrated that it is advantageous to consider batches of a limited number of forward and adjoint histories and to process all possible combinations of collision sites only within one batch. There is also a possibility of optimising the number of adjoint histories relative to the number of forward histories within a batch.

Another way of improving the efficiency of the calculation is to conditionally accept pairs of forward and adjoint collision sites. If the collision sites to be coupled are far away from each other, the score will be small because of the exponential attenuation in the estimators. Hence, such pairs of collision sites can be

subjected to a kind of Russian roulette before they are accepted, in which case the score is multiplied by the inverse of the acceptance probability.

A general problem with the next-event estimator for a point detector is its $1/r^2$ character, which leads to an unbounded estimator if the two positions are very near to each other. The $1/r^2$ term is also present in the estimator of Eq.(36). However, in our case the forward collision site is always in volume V_S and the adjoint collision site is always in volume V_D. Hence, the estimator becomes only unbounded when both collision sites are very close to the separating surface A. This is more unlikely than that a collision sites is very close to a point detector. In our numerical examples we could not detect any problem with the $1/r^2$ character of the estimator.

There are other methods of coupling a forward and an adjoint Monte Carlo calculation. With respect to the midway coupling method discussed before[3] the current method has the advantage that no discretization at the intermediate surface is necessary and remains therefore without approximations. Another way is the correlated coupling method[6], in which the forward and adjoint particle start at the same position at the intermediate surface with the same energy and direction and give a score when they reach the source and detector, respectively. This will lead to efficiency problems if the source and/or the detector are small. In the next-event coupling method the source and the detector can be even a point in space without any problem.

REFERENCES

1. S. Cramer, "The Evaluation of Radiation Transport Forward-Adjoint Flux Integral Using Monte Carlo Correlated Coupling Methods", *Nucl. Sc. Eng*., to appear.
2. T. Ueki, J.E. Hoogenboom and J.L. Kloosterman, "Monte Carlo Forward-Adjoint Coupling by Next Event Estimation", *M&C99*, Madrid, September 1999, pp. 241-250.
3. I.V. Serov, T.M. John and J.E. Hoogenboom, "A Midway Forward-Adjoint Coupling Method for Neutron and Photon Monte Carlo Transport", *Nucl. Sc. Eng.* **133**, pp. 55-72 (1999).
4. J.E. Hoogenboom, "Methodology of Continuous Energy Adjoint Monte Carlo for Neutron, Photon and Coupled Neutron-Photon Transport", submitted to *Nucl. Sc. Eng*.
5. G.I. Bell and S. Glasstone, *Nuclear Reactor Theory*, Van Nostrand, New York (1971).
6. T. Ueki, J.E. Hoogenboom and J.L. Kloosterman, "Analysis of Correlated Coupling of Monte Carlo Forward and Adjoint Histories", *Nucl. Sc. Eng.* **137**, pp. 117-145 (2001).